On the joint distribution of excursion duration and amplitude of a narrow-band Gaussian process

Ghane, Mahdi; Gao, Zhen; Blanke, Mogens; Moan, Torgeir

Published in:
IEEE Access

Link to article, DOI:
10.1109/ACCESS.2018.2816600

Publication date:
2018

Document Version
Publisher's PDF, also known as Version of record

IEEE Access
Multidisciplinary | Rapid Review | Open Access Journal

Received December 28, 2017, accepted March 10, 2018, date of publication March 16, 2018, date of current version April 4, 2018.

Digital Object Identifier 10.1109/ACCESS.2018.2816600

On the Joint Distribution of Excursion Duration and Amplitude of a Narrow-Band Gaussian Process

MAHDI GHANE[1,2], ZHEN GAO[1,2], MOGENS BLANKE[2,3], (Senior Member, IEEE), AND TORGEIR MOAN[1,2]

[1]Center for Ships and Ocean Structures, Department of Marine Technology, Norwegian University of Science and Technology, 7491 Trondheim, Norway
[2]Center for Autonomous Marine Operations and Systems, Department of Marine Technology and Department of Engineering Cybernetics, Norwegian University of Science and Technology, 7491 Trondheim, Norway
[3]Department of Electrical Engineering, Technical University of Denmark, 2800 Lyngby, Denmark

Corresponding author: Mahdi Ghane (mahdi.ghane@ntnu.no)

This work has been carried out at the Center for Autonomous Marine Operations and Systems (AMOS) and Center for Ships and Ocean Structures (CeSOS). The Norwegian Research Council is acknowledged as the main sponsor through the Centers of Excellence Funding Scheme, Project numbers 146025-CeSOS and 223254-AMOS.

ABSTRACT The probability density of crest amplitude and duration that exceeds a given level is used in many theoretical and practical problems in engineering that are subjected to fluctuating loads such as wind and wave loads. The presently available joint distributions of amplitude and period are limited to excursion through a mean-level or to describe the asymptotic behavior of high level excursions. This paper extends the knowledge by presenting a theoretical derivation of probability of wave exceedance amplitude and duration for a stationary narrow-band Gaussian process. A density function is suggested that has the salient feature to depend only on the three lowest spectral moments m_0, m_1, *and* m_2 and desired level of exceedance, H. It does not require any condition on the autocorrelation function. This paper shows how increase in H, increases the correlation between excursion periods and amplitude. This paper also shows that how the accuracy of the proposed joint distribution relates to spectral width parameter, ν, and that accuracy increases for higher levels of H, especially for a spectrum describing a physical phenomenon such as a sea state spectrum. It was demonstrated that the marginal distribution of amplitude is Rayleigh distributed, as expected, and that the marginal distribution of excursion duration works for asymptotic and non-asymptotic levels. Results demonstrate that the established distribution fits well with ideal narrow-band Gaussian processes as well as the sea states at three European sites —in the Atlantic Ocean and the North Sea. The suggested model is found to be a good replacement for the existing empirical distributions.

INDEX TERMS Stationary process, Gaussian narrow-band process, joint distribution, excursion duration, crest amplitude, level crossing.

I. INTRODUCTION

The probability distribution function (PDF) of amplitude and duration of exceeding a certain level of a stochastic process, $\zeta(t)$, is essential for many theoretical and practical problems. These range from mechanical stress analysis, change detection problems, fading phenomena in wireless communication and many applications in marine, offshore and coastal engineering. In offshore and coastal engineering, it includes both short-term and long-term statistics. Short-term applicability includes slamming loads, deck-impact events, short-term probability distribution of impact duration, bottom-slam forces, over-topping waters for wave breakers and wave energy convertors [1]. Long-term application includes operation, installation and survival of offshore renewable energy and platforms in general [2], [3].

Investigating of the distribution of amplitude (maxima) and period dates back to the the pioneer works of Rice [4], [5]. He scrutinized the statistical properties of a random function —noise in an electrical circuit—and established a closed-form expression, i.e., the Rice formula, of the average crossing rate under favorable conditions. By using the average crossing rate, he derived the distribution of maxima for a

Gaussian process. His fundamental results were summarized in [2] and [6]. Wave period can be defined as the time between two successive local maxima or successive up-crossing through the mean level. Opting the latter definition, various approximations of wave period density functions have been proposed, for example, Rice [4], [5, Sec. 3.4] and Longuet-Higgins [7]–[9].

The probability density of excursion (exceedance) duration, time between an level-up-crossing followed by a level-down-crossing, were also derived by Rice [5]. The proposed approach is, however, rather complicated for non-zero levels and can only be estimated by means of demanding numerical integration. Non-diagonal covariance matrix between stochastic function and its derivative hinders a simple analytical derivation of the density of excursion duration. Many researchers, therefore, tried to address this issue by approximating the integration. By partitioning an n-dimensional normal space to subspaces, Wu-Zhou and Ming-Shun [10] proposed a semi-analytic method to reduce the computational efforts. Empirical parametric models for the duration statistics of the significant wave height were established by Graham [11], and Kuwashima and Hogben [12].

Analytical expressions for the mean value and variance of excursion duration can be found in [13] and [14], where Mathiesen [14] used the mean value expression to validate a empirical parametric model. A number of researchers have treated this problem by assuming an asymptotically large level of excursion [15]–[21]. Using orthogonal series, Gram-Charlier, Edgeworth or Laguerre series, is another approach to approximate the PDF of exceedance and non-exceedance duration [3].

The joint distribution of wave period and amplitude is a more challenging problem in the most general case. However, for a stochastic process with a narrow-band spectrum some simplifications can be made; Wooding [22] was the first to derive the joint distribution of wave amplitude and period for a narrow-band spectrum using the density of the wave envelope and its time derivative. Cavanie *et al.* [23] proposed a closed-form expression for the joint distribution assuming a narrow-band Gaussian random process based on spectral moments up to 4th order (m_0, m_1, m_2, m_4). By extracting the mean frequency of the spectrum, Longuet-Higgins [24], [25] ended up with a diagonal covariance matrix between slow-varying envelope, high-frequency component and their time derivatives, and derived a simpler closed-form expression for the joint distribution of wave period and amplitude based on spectral moments (m_0, m_1, m_2). Using the joint distribution established by Longuet-Higgins, EM. Antao and CG. Soares proposed the joint distribution of wave steepness in narrow-band sea states [26]. However, these closed-form formulas cannot provide a description of the joint density of amplitude and excursion duration nor density of excursion duration for a level that differs from the mean level.

To the best knowledge of the authors, there is no closed-form expression for the joint distribution of excursion period and amplitude yet. Hence, the objective of this paper is to fill this gap and establish a closed-form expression for the joint distribution of exceedance duration and amplitude above a certain level and parameterize this with low-order spectral moments. We assume a Gaussian narrow-band process with continuous first derivative. The paper will also show how the the empirical excursion distribution model can be replaced by the marginal distribution for excursion duration that follows from the joint distribution. The paper will validate the suggested closed-form joint distribution with simulated ideal narrow-band and sea states data and investigate the accuracy of the model when the bandwidth of the underlying narrow-band process changes towards a broader bandwidth stochastic process and for different levels.

The remainder of this paper is organized as follows. Section II presents a derivation of the joint distribution of excursion duration and amplitude and determines the marginal distribution of amplitudes and excursion duration. Section III validates the model using the simulation results from ideal-narrowband spectra and sea states data. The Kolmogorov-Smirnov test (K-S test) is used as a goodness-of-fit (GoF) test to provide a quantitative measure of the accuracy of the suggested joint distribution. Finally, Section IV concludes and highlights the main findings of the paper.

II. STATEMENT OF THEORETICAL RESULTS

A. ASSUMPTIONS

A Gaussian random process $\zeta(t)$—any function indexed by time representing for example the wave elevation at a specific point in space—has been commonly been represented by the Fourier series Eq. (1), [24], [25], [27], [28].

$$\zeta(t) = \sum_{n=1}^{\infty} a_n cos(\omega_n t + \epsilon_n) \tag{1}$$

Where a_n and ϵ_n are statistically independent random variables. The amplitude a_n is Rayleigh distributed, and the phase ϵ_n is uniformly distributed over $[0, 2\pi)$. For a narrow-band process, ω_n is densely distributed over $(0, \infty)$. A narrow-band assumption helps to break down $\zeta(t)$ into a carrier high frequency wave with the mean frequency $\overline{\omega}$, and a slowly varying envelope function Eq. (2), [24], [25].

$$\zeta(t) = Rel\left\{\rho e^{i\phi} e^{i\bar{\omega}t}\right\}, \tag{2}$$

where $\rho e^{i\phi}$ is the complex-value envelope function of time t and total phase ϕ Eq. (3),

$$\rho e^{i\phi} = \sum_{n=1}^{\infty} a_n \exp\{i[(\omega_n - \bar{\omega}) + \epsilon_n]\}. \tag{3}$$

The mean frequency $\bar{\omega}$ is defined as:

$$\bar{\omega} = \frac{m_1}{m_0}, \tag{4}$$

where m_n stands for the *nth* central moment of the spectral density $S(\omega)$ of $\zeta(t)$:

$$m_n = \int_0^{\infty} w^n S(\omega) d\omega. \tag{5}$$

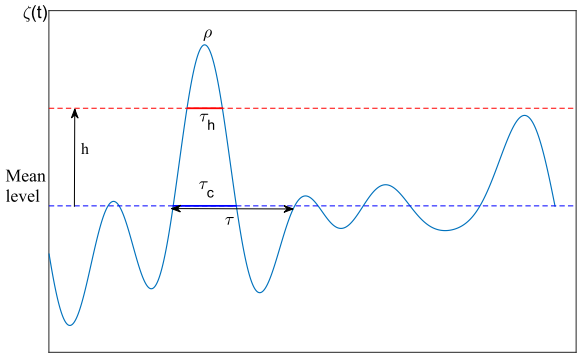

FIGURE 1. Relation between exceedance duration τ_h –for given level h–crest amplitude ρ, crest period τ_c and wave period τ.

Similarly the nth non-central moment of the spectral density $S(\omega)$ is defined as:

$$\mu_n = \int_0^\infty (w - \bar{w})^n S(\omega) d\omega, \tag{6}$$

and spectral width parameter ν is defined as

$$\nu^2 = \frac{\mu_2}{\bar{\omega}^2 m_0}. \tag{7}$$

Longuet-Higgins [24], [25] derived the closed-form joint distribution for a narrow-band ($\nu^2 \leq 0.36$) Gaussian process which has a continuous first derivative, Eq. (8).

$$p(A_c, T) = \frac{2}{\nu \pi^{1/2}} L(\nu) \frac{A_c^2}{T^2} exp\left\{-A_c^2\left[1+(1-1/T)^2 \nu^{-2}\right]\right\} \tag{8}$$

Where A_c and T represent the normalized crest amplitude and period, respectively. The crest amplitude, ρ, is normalized by $\sqrt{2\, m_0}$ and wave period, τ, time between two successive zero-up-crossing, is normalize by the mean period $\bar{\tau}$, Eq. (9), Fig. 1.

$$A_c = \frac{\rho}{(2m_0)^{\frac{1}{2}}}, \quad T = \frac{\tau}{\bar{\tau}}, \ \bar{\tau} = \frac{2\pi m_0}{m_1}. \tag{9}$$

$L(\nu)$ is a function of spectral width parameter ν and defined as

$$L(\nu) = \frac{2}{\left[1 + \left(1 + \nu^2\right)^{-1/2}\right]}. \tag{10}$$

B. DERIVATION OF THE JOINT DISTRIBUTION OF EXCURSION DURATION AND AMPLITUDE

Starting from Longuet-Higgins joint distribution of amplitude and period, Eq. (8), and assuming that zero-up-up crossing period T is twice the zero-up-down crossing period T_c, we end up with the joint distribution of the crest period and amplitude, Eq. (11).

$$p(A_c, T_c) = \frac{1}{\nu\sqrt{\pi}} L(\nu) \frac{A_c^2}{T_c^2} \times exp\left\{-A_c^2\left[1 + (1 - 1/2T_c)^2 \nu^{-2}\right]\right\} \tag{11}$$

For a narrow-band process where there is only one maxima between two successive zero-up-down crossing a sine-shape function can be used to approximate the relation between the crest amplitude (greater than a given threshold), the crest period and the excursion duration, Fig. 1.

The total phase, $\Delta phase$, pertinent to excursion time is presented in Eq. (12), approximating the phase ϕ using a sine-shape function. Eq. (15) presents the relation between normalized excursion duration T_H, crest period T_c and crest amplitude A_c.

$$\left\{\begin{array}{c} \rho\, sin(\phi) = h \\ \rho\, sin(\pi - \phi) = h \end{array}\right\} \Rightarrow \pi - 2\phi = \Delta phase \Rightarrow \pi - 2\phi = \frac{\pi}{\tau_c}\tau_h \tag{12}$$

$$\tau_h = \left(1 - \frac{2}{\pi} arcsin\left(\frac{h}{\rho}\right)\right)\tau_c \quad \xrightarrow{Normalizing} \tag{13}$$

$$\frac{\tau_h}{\bar{\tau}} = \left(1 - \frac{2}{\pi} arcsin\left(\frac{\frac{h}{\sqrt{2m_0}}}{\frac{\rho}{\sqrt{2m_0}}}\right)\right)\frac{\tau_c}{\bar{\tau}} \Rightarrow \tag{14}$$

$$T_H = \left(1 - \frac{2}{\pi} arcsin\left(\frac{H}{A_c}\right)\right) T_c. \tag{15}$$

Introducing an auxiliary variable such as y, we now convert A_c, T_c domain to y, T_H domain Eqs. (16) to (18)

$$p(A_c, T_c) \xrightarrow{\text{change of variables}} \times \left\{\begin{array}{c} y = A_c := g_1(A_c, T_c) \\ T_H = \left(1 - \frac{2}{\pi} arcsin\left(\frac{H}{A_c}\right)\right) T_c := g_2(A_c, T_c) \end{array}\right\} \tag{16}$$

$$\Rightarrow \left\{\begin{array}{c} A_c = g_1^{-1}(T_H, y = A_c) \\ T_c = \frac{T_H}{\left(1 - \frac{2}{\pi} arcsin\left(\frac{H}{A_c}\right)\right)} = g_2^{-1}(T_H, A_c) \end{array}\right\} \tag{17}$$

$$\begin{aligned} p(A_c, T_H) &= p_{A_c, T_c}\left(g_1^{-1}, g_2^{-1}\right) \times |J| \\ &= \frac{1}{\nu\sqrt{\pi}} L(\nu) \frac{A_c^2}{T_H^2}\left(1 - \frac{2}{\pi} arcsin\left(\frac{H}{A_c}\right)\right) \\ &\quad \cdot exp\left\{-A_c^2\left[1 + \left(1 - \frac{\left(1 - \frac{2}{\pi} arcsin\left(\frac{H}{A_c}\right)\right)}{2T_H}\right)^2 \nu^{-2}\right]\right\}. \end{aligned} \tag{18}$$

In order to obtain a simpler form of Eq. (18) over the desired domain, $\frac{H}{A_c} \in [0, 1]$ interval, we approximate as follows

$$\left(1 - \frac{2}{\pi} arcsin\left(\frac{H}{A_c}\right)\right) \simeq \sqrt{1 - \frac{H}{A_c}}; \quad \text{for } \frac{H}{A_c} \in [0, 1] \tag{19}$$

Fig. 2 depicts this approximation. It is seen that the Taylor expansion (even up to 5th order) cannot capture the $\left(1 - \frac{2}{\pi} arcsin\left(\frac{H}{A_c}\right)\right)$ function when $\frac{H}{A_c}$ goes toward one.

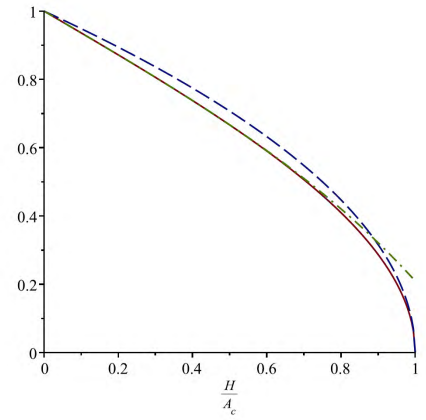

FIGURE 2. $\left(1-\frac{2}{\pi}arcsin\left(\frac{H}{A_c}\right)\right)$ **(solid line), and its Taylor expansion up to 5th order (dash-dot line), and** $\sqrt{1-\frac{H}{A_c}}$ **(dashed line).**

$\sqrt{1-\frac{H}{A_c}}$ function, however, seems to be a better and simpler approximation for all the desired range. The ensuing simpler form is also helpful to handle the integrations in order to derive marginal distributions. We, therefore, end up with the following form for the joint distribution of crest amplitude and excursion duration for a given threshold level H, Eq. (20).

$$p(A_c, T_H) = K(H,\nu)\frac{1}{\nu\sqrt{\pi}}\,L(\nu)\,\frac{A_c^2}{T_H^2}\sqrt{1-\frac{H}{A_c}} \cdot \exp\left\{-A_c^2\left[1+\left(1-\frac{\sqrt{1-\frac{H}{A_c}}}{2T_H}\right)^2\nu^{-2}\right]\right\} \tag{20}$$

Where $L(\nu)$ is the same as Eq. (10). We also need to add a normalization factor, say $K(H,\nu)$, to guarantee that $\int\int (A_c, T_H)\, dA_c dT_H$ is unity. Where $K(H,\nu)$ clearly depends on H and ν values and will be addresed in Section II-C and Appendix. IV-B. The joint distribution $p(A_c, T_H)$ for $\nu = 0.5$ and for different normalized threshold $H = [0, 0.5, 1, 2]$ are depicted in Fig. 3. Each contour represents a quantile level enclosing P% of the probability density function while P takes the values 10, 30, 50, 70, 90, 95 and 99 from the center contour outwards. The established joint density function works both for zero and non-zero level H, and for $H = 0$, it produce the similar result as was presented by Longuet-Higgins [25]. As H increases, we end up with a narrower distribution especially with respect to excursion duration, Figs. 3b to 3d. It should be noted that the result for narrower spectrum (smaller ν values) are similar. It is evident, as previously also shown in other literature [23]–[25] for $H = 0$, the smaller the ν values are, the narrower the excursion duration are for the same threshold level H.

C. THE MARGINAL DISTRIBUTION OF $p(A_c)$ FOR $A_c > H$

In order to derive the density of wave crest amplitude A_c, we need to integrate $p(A_c, T_H)$ with respect to T_H over $0 <$

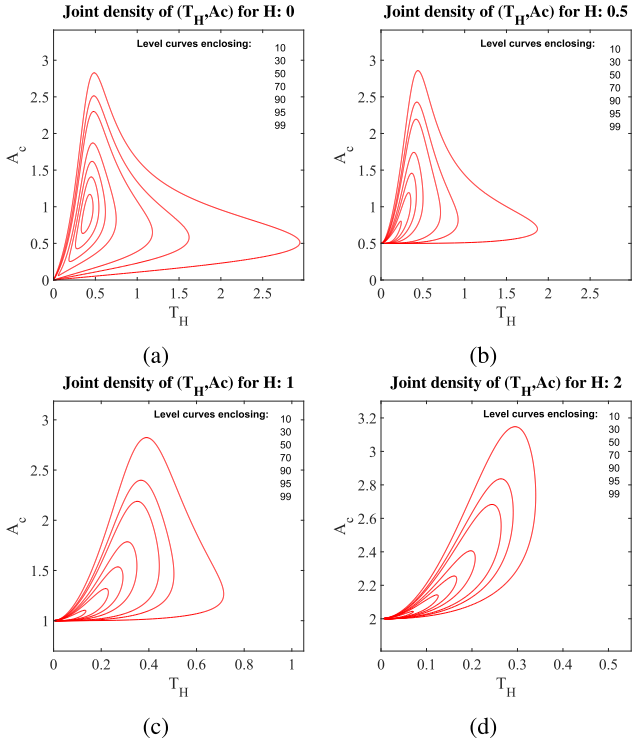

FIGURE 3. **Contour lines of the joint density of normalized excursion duration (T_H) and normalized crest amplitude (A_c) for Gaussian process for $\nu = 0.5$ and for different normalized level $H = [0, 0.5, 1, 2]$, where contours represent quantile levels which enclose P% of the PDF and P takes [10, 30, 50, 70, 90, 95, 99] values from center contour outwards.**

$T_H < \infty$,

$$p(A_c) = \int_0^\infty p(A_c, T_H)dT_H = K(H,\nu)\frac{1}{\nu\sqrt{\pi}}\,L(\nu)\,\frac{A_c^2}{1}\sqrt{1-\frac{H}{A_c}}\exp\left(-A_c^2\right) \cdot \int_0^\infty \frac{1}{T_H^2}\exp\left\{\left(\frac{A_c}{\nu}\right)^2\left(1-\frac{0.5\sqrt{1-\frac{H}{A_c}}}{T_H}\right)^2\right\}dT_H. \tag{21}$$

The integral part can be written as

$$\int_0^\infty \frac{1}{T_H^2}\exp\left\{-a^2\left(1-\frac{b}{T_H}\right)^2\right\}dT_H, \tag{22}$$

where a is $\frac{A_c}{\nu}$ and b is $0.5\sqrt{1-\frac{H}{A_c}}$. By applying $\beta = a\,(1 - b/T_H)$, we end up with the same results as Longuet-Higgins [25], Eq. (23), where he only considered the case where H was zero.

$$A_c\exp(-A_c^2)\,L\,(\nu)\,\frac{2}{\sqrt{\pi}}\int_{-\infty}^{\frac{A_c}{\nu}}\exp\left(-\beta^2\right)d\beta = A_c\exp(-A_c^2)\,L\,(\nu)\left[1+\mathrm{erf}(\frac{A_c}{\nu})\right] \tag{23}$$

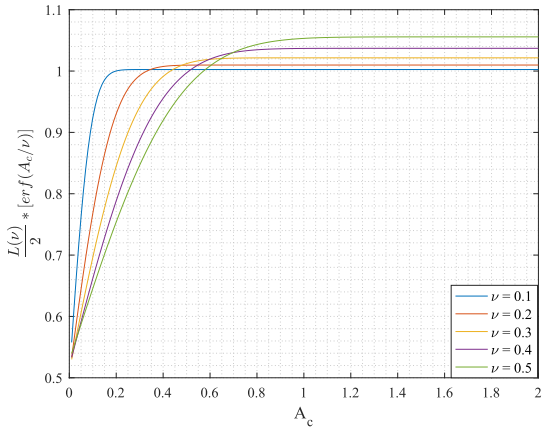

FIGURE 4. The value of $\frac{L(\nu)}{2}\left[1+\text{erf}(\frac{A_c}{\nu})\right]$ for different values of $\nu = [0.1, 0.2, 0.3, 0.4, 0.5]$.

The only difference, as the general form —H is not necessarily zero—is that for $A_c < H$, $p(A_c)$ is zero; accordingly the distribution of crest amplitude $p(A_c)$ is

$$\begin{cases} K(H,\nu)\, 2A_c \exp(-A_c^2)\, \frac{L(\nu)}{2}\left[1+\text{erf}(\frac{A_c}{\nu})\right] & \text{for } A_c > H \\ 0 & \text{for } A_c < H \end{cases} \tag{24}$$

Setting $A_c = r/\sqrt{2}$, $2\,A_c \exp(-A_c^2)$ becomes $r\exp(-\frac{r^2}{2})$ which is, as we expected, the Rayleigh distribution. We need also to consider a normalization factor, $K(H,\nu)$, to take into account the effect of $\frac{L(\nu)}{2}\left[1+\text{erf}(\frac{A_c}{\nu})\right]$ coefficient. Fig. 4 evaluates $\frac{L(\nu)}{2}\left[1+\text{erf}(\frac{A_c}{\nu})\right]$ for different values of ν and A_c.

It is seen that for small ν and large A_c values, $\frac{L(\nu)}{2}\left[1+\text{erf}(\frac{A_c}{\nu})\right]$ is close to unity. For this especial case, by assuming $\frac{L(\nu)}{2}\left[1+\text{erf}(\frac{A_c}{\nu})\right] = 1$, Longuet-Higgins showed that normalization factor, $K(H,\nu)$, is equal to $\exp(H^2)$, [25]. Accordingly, Fig. 5 shows the density function of crest amplitude A_c which is almost Rayleigh distributed, yet it must be corrected by a factor of $\frac{L(\nu)}{2}\left[1+\text{erf}(\frac{A_c}{\nu})\right]$. It is seen that $p(Ac)$ goes towards a Rayleigh distribution by increasing A_c and by decreasing ν values, narrower spectrum. It should be noted that dash-line is referred to Rayleigh distribution shape —the Rayleigh distribution—since its integral is not unity. It is scaled with $\exp(H^2)$ for comparison.

The general form of the normalization factor, $K(H,\nu)$ in Eq. (24) is derived in the Appendix. IV-B, and is presented in Eq. (25).

$$K(H,\nu) = \frac{1+\sqrt{\nu^2+1}}{1+\exp\left(-H^2\right)\sqrt{\nu^2+1}\left(1+\text{erf}\left(\frac{H}{\nu}\right)\right)-\text{erf}\left(\frac{H\sqrt{\nu^2+1}}{\nu}\right)}, \tag{25}$$

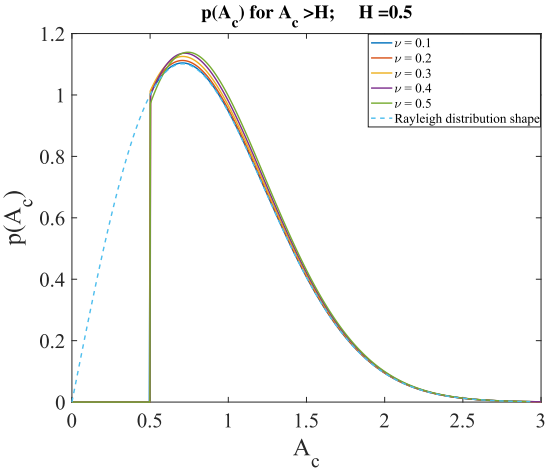

FIGURE 5. The density of crest amplitude, A_c, larger than threshold H, for $\nu = [0.1, 0.2, 0.3, 0.4, 0.5]$ and Rayleigh distribution shape.

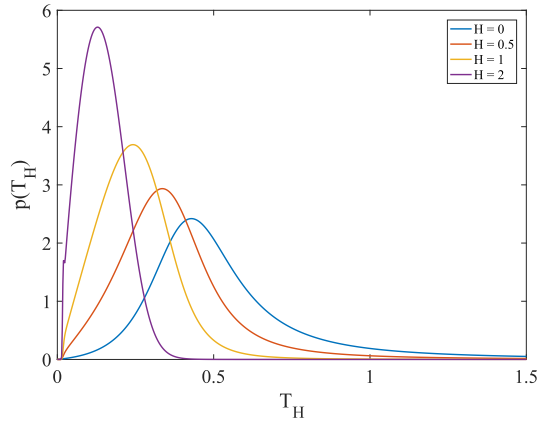

FIGURE 6. The density of the excursion duration, T_H, for $\nu = 0.5$ and for different threshold $H = [0, 0.5, 1, 2]$.

D. THE MARGINAL DISTRIBUTION OF $p(T_H)$

The density distribution of T_H, is obtained by integrating $p(A_c, T_H)$ with respect to A_c over $H < A_c < \infty$. The desity of T_H for $H = 0$, which is the crest period T_c, was derived by Longuet-Higgins [25]. However, for the general case $H > 0$, the analytic closed-form solution is possible to obtain but too long and too complicated; hence, the numerical integration is adopted here, Fig. 6.

Fig. 6. is the numerical projection of Fig. 3 with respect to T_H dimension. It is seen that, increasing normalized threshold H results in a narrower density of T_H. Smaller ν values, similarly, result in narrower density of T_H.

As it was shown in [25] the mean value of the T_H distribution is theoretically infinite for $H = 0$, since for asymptotic value of T_c the density $p(T_c)$ behaves like T_c^{-2} function; therefore, an alternative estimate of the mean period was adopted for normalization. We use the same approach and extend it for the general case i.e. $H \geq 0$.

As it can be deducted from Fig. 7, for a random process like $\zeta(t)$ and given a threshold H, expected value of the excursion

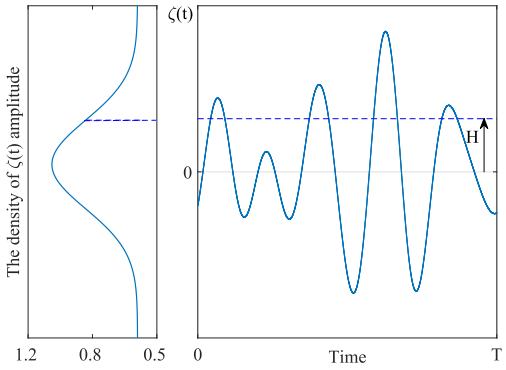

FIGURE 7. Schematic for expected value of excursion duration.

period $E[T_H]$, as an alternative approach, is presented in Eq. (26), [13], [14], [29].

$$E\left[T_H\right] = \frac{\left[Pr(\zeta(t) \geq H)\right] T}{N^{+}(T, H)} \tag{26}$$

Where $[Pr(\zeta(t) \geq H)]\,T$ represents all time $\zeta(t)$ spends above the threshold, and $N^{+}(T, H)$ represents number of positive-level H crossing during T time span, Fig. 7. For a Gaussian process, accordingly, we have

$$Pr\left(\zeta(t) \geq H\right) = \frac{1}{2}\left[1 - \text{erf}\left(\frac{H}{\sqrt{2m_0}}\right)\right], \tag{27}$$

and based on the Rice formula for a Gaussian process [4] and [5] we have

$$\frac{N^{+}\left(T, H\right)}{T} = \frac{1}{2\pi}\sqrt{\frac{m_2}{m_0}}\exp\left(\frac{-H^2}{2m_0}\right). \tag{28}$$

Therefore,

$$E\left[T_H\right] = \left[1 - \text{erf}\left(\frac{H}{\sqrt{2m_0}}\right)\right]\pi\sqrt{\frac{m_0}{m_2}}\exp\left(\frac{H^2}{2m_0}\right). \tag{29}$$

Replacing $H = 0$ in Eq. (29), we end up with half the same value as derived by Longuet-Higgins [25], the 0.5 coefficient is because he assumed a period as time between two successive zero-up crossing and we consider the crest period which is half the period. Hence, we modify the $p(T_H)$ using the following correction coefficient for the T_H

$$\frac{E\left[T_H\right]}{\overline{T}_H} \tag{30}$$

where $\overline{T}_H$ is obtained from marginal distribution, $p(T_H)$, Eq. (20). The proposed modification helps to provide a more accurate estimation of the distribution of excursion duration.

III. COMPARISON WITH IDEAL NARROW-BAND GAUSSIAN PROCESS AND REAL SEA STATES

To provide a simulation-based validation for the proposed joint distribution of excursion duration and crest amplitude, three approaches are adopted. First, ideal narrow-band spectrum is constructed, for $\nu = [0.1, 0.2, 0.3, 0.4, .5]$ —$\nu = 0.6$ is excluded for reasoning see Appendix. IV-A. Then, time series realization are generate with more than 1e+6 sample point in time domain for different levels. Obtained excursion duration and crest amplitudes from simulation are, then, compared with theoretical results established in the paper. Second, real sea states are used to compare the efficiency of the proposed formula for spectra describing physical phenomenon. Finally, Kolmogorov-Simirnov (K-S) test as a goodness of fit (GoF) test is chosen to provide a quantitative metrics to scrutinize statistical sensitivity in different regions of the proposed PDFs.

Fig. 8 depicts the stepwise simulation for a narrow-band Gaussian process. Part (a) shows an ideal spectral density for $\nu = 0.3$ and $\bar{w} = 0.6$; a small portion of the related time-domain realization is depicted in part (b). Black dots in part (c) represents the normalized crest amplitudes for $A_c > 0.5$ and related normalized excursion duration that are obtained form time-domain realization. Green contours show their Kernel density estimation (KDE) for the joint distribution of excursion duration and crest amplitude. The KDE provides a non-parametric piecewise approximation of the joint distribution to compare with the established PDF. Each contour represents a quantile level enclosing P% of the PDF while P takes the 10, 30, 50, 70, 90, 95 and 99 values from the center contour outwards. Part(d) is like part (c), while contours are obtained from the proposed analytic expression in this paper Eq. (20). It is seen that the KDE and established formula are matched pretty well. Parts (e) shows the PDF of the normalized crest amplitude (solid line), Eq. (24), while dashed-line represents the scaled Rayleigh distribution for a better comparison. Part (f) shows the cumulative distribution function (CDF) of both empirical data and analytic approach; CDF gives a better appreciation of accumulation of error between numerical simulation and proposed analytic formula. Part (g) shows the marginal distribution of the excursion duration, $p(T_H)$, accommodating the correction factor, Eq. (30). Similarly, $CDF(T_H)$ is shown in (h). Simulation data and proposed closed-form formula for the $p(A_c, T_H)$ and its marginal distributions, i.e, $p(T_H)$ and $p(A_c)$ agree well with each other, Fig. 8.

It is intended to show the trend both with respect to change of ν and H values. To save spaces, only a few figures are shown; more comparison is presented later on using K-S test. Fig. 9 depicts similar results for $\nu = 0.5; H = 0.5$ values to investigate the change of spectral width parameter ν. For a given mean frequency, here $\bar{w} = 0.6$, by increasing ν value we should expect a wider spectrum which is also appreciated from time-domain realization, i.e., occasionally having more than one maxima between each zero-up crossing and the next zero-down crossing, which contradict our assumptions—narrow-band assumption and using a sine shape function to approximate change of phase for a given threshold level H. Accordingly, we should expect a decrease in the performance of the proposed joint distribution and density of excursion duration for $\nu = 0.5$, Fig. 9(h).

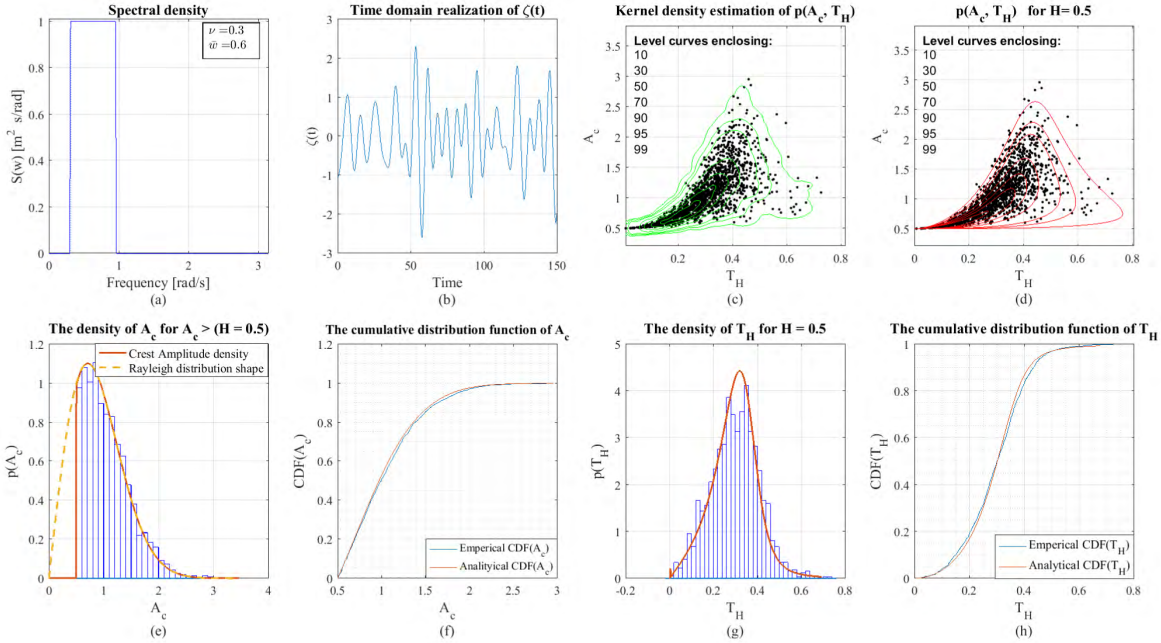

FIGURE 8. Time domain simulation of an ideal narrow-band Gaussian process for $\nu = 0.3$ and normalize threshold $H = 0.5$; (a) depicts the spectral density, (b) is a portion of the related time domain realization; black dots in (c) are crest amplitudes greater than H and related excursion duration and green curves are the obtained kernel density estimation of $p(A_c, T_H)$; (d) shows the proposed theoretical formula for $p(A_c, T_H)$ Eq. (20); (e:f) are the marginal distributions for crest amplitude and excursion period, respectively.

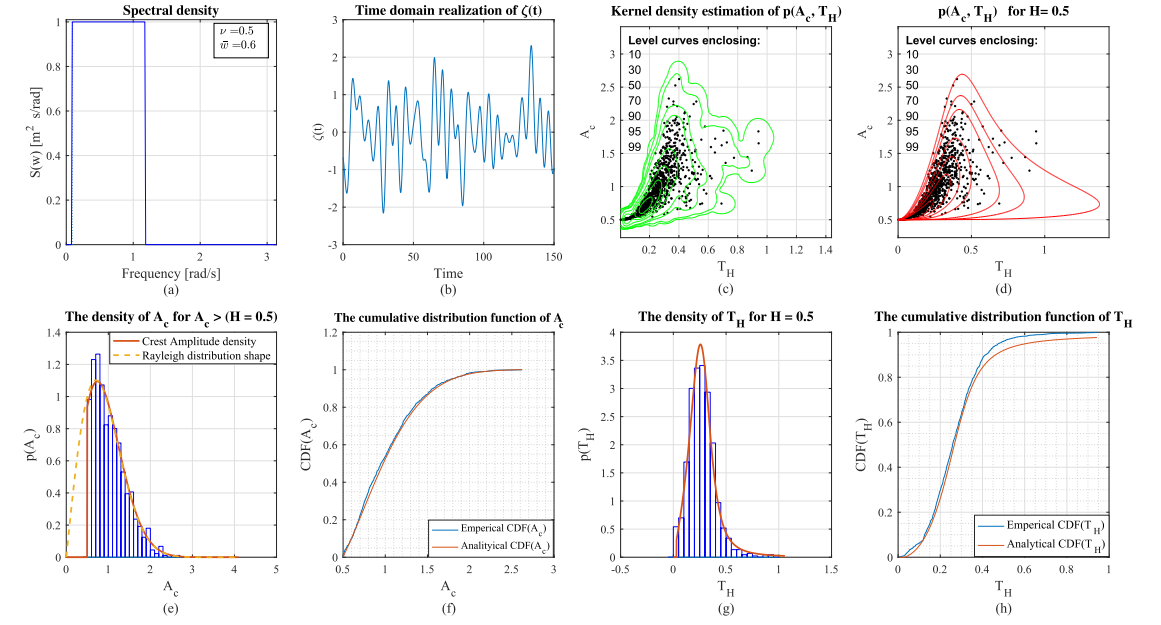

FIGURE 9. Time domain simulation of an ideal narrow-band Gaussian process for $\nu = 0.5$ and a normalized threshold $H = 0.5$. (a) Depicts the spectral density, (b) is a portion of the related time domain realization; black dots in (c) are crest amplitudes greater than H and related excursion duration and green curves are the obtained kernel density estimation of $p(A_c, T_H)$; (d) shows the proposed theoretical formula for $p(A_c, T_H)$ Eq. (20); (e:f) are the marginal distributions for crest amplitude and excursion period, respectively.

Figs. 10 and 11 depicts the similar simulation results for $\nu = 0.5$; $H = [1, 2]$. Trend for higher H values is similar to smaller ν values —narrower spectrum. That is, the excursion duration decreases by increasing H values, which results in narrower distribution of both amplitude and excursion duration. This is appreciable from visual comparison between Figs. 8, 10 and 11. It is seen that the proposed joint distribution and the marginal distributions for crest amplitude and excursion duration matches well, except for $\nu = 0.5$ and $H = 0.5$, with the simulation data even for a quiet wide spectrum, i.e., $\nu = 0.5$.

Sea states simulations, as examples of physical phenomenon comparing to ideal narrow-band spectra, are carried out for three different European offshore sites in Atlantic

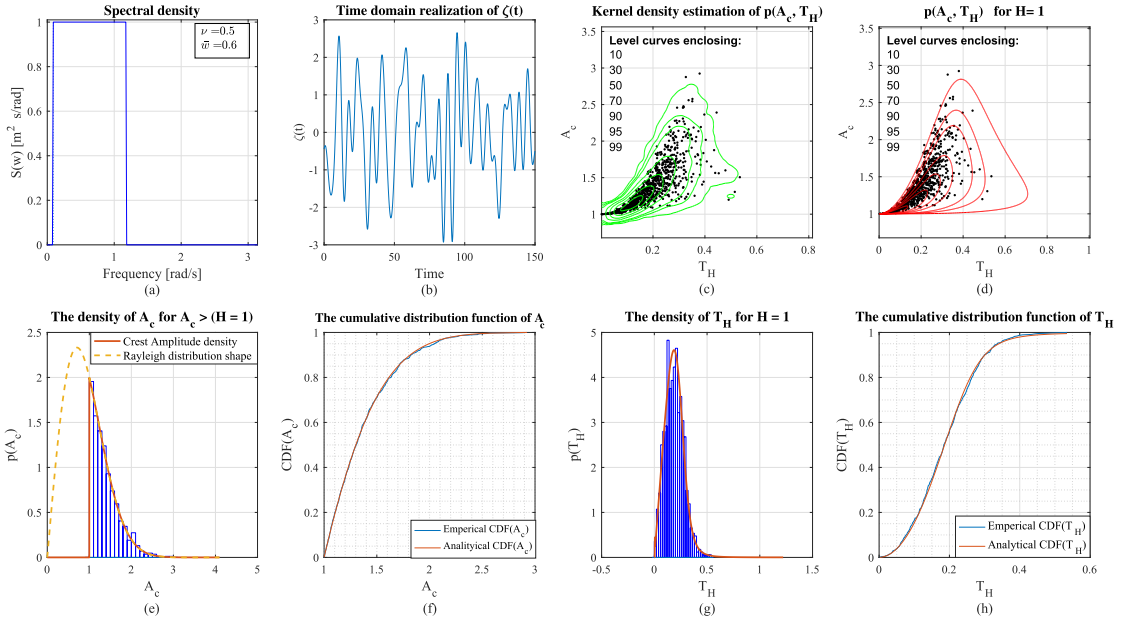

FIGURE 10. Time domain simulation of Ideal narrow-band Gaussian process for $\nu = 0.5$ and normalize threshold $H = 1$. (a) depicts the spectral density, (b) is a portion of the related time domain realization; black dots in (c) are crest amplitudes greater than H and related excursion duration and green curves are the obtained kernel density estimation of $p(A_C, T_H)$; (d) shows the proposed theoretical formula for $p(A_C, T_H)$ Eq. (20); (e:f) are the marginal distributions for crest amplitude and excursion period, respectively.

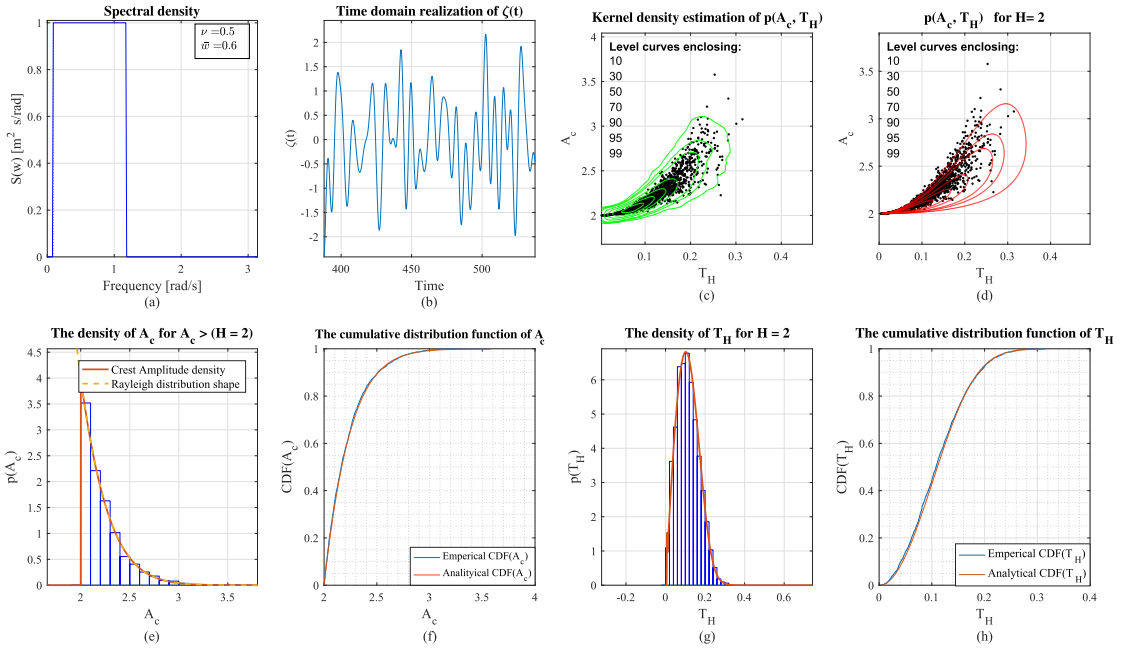

FIGURE 11. Time domain simulation of Ideal narrow-band Gaussian process for $\nu = 0.5$ and normalize threshold $H = 2$. (a) depicts the spectral density, (b) is a portion of the related time domain realization; black dots in (c) are crest amplitudes greater than H and related excursion duration and green curves are the obtained kernel density estimation of $p(A_C, T_H)$; (d) shows the proposed theoretical formula for $p(A_C, T_H)$ Eq. (20); (e:f) are the marginal distributions for crest amplitude and excursion period, respectively.

ocean and North sea, [30]. The related critical conditions obtained from 50-year record. General information and statistics of the sites is shown in Table 1. Due to similarity, only simulation results for site No.1 are presented in this section, the detailed results for GoF test statistics for all three sites and for different threshold level H are presented later in the paper. Time realizations are generated with wave conditions characterized by significant wave height $H_S = 8\ m$ and

TABLE 1. General information of three european sites.

Site No.	Area	Name	Water depth [m]	Distance to shore [km]	Hs [m]	Tp [s]
1	Atlantic; French coast	Sem Rev	33	15	8	12
2	North sea; Norway	Norway 5	202	30	13.5	13
3	North sea; Norway	North Sea Center	29	300	8	10

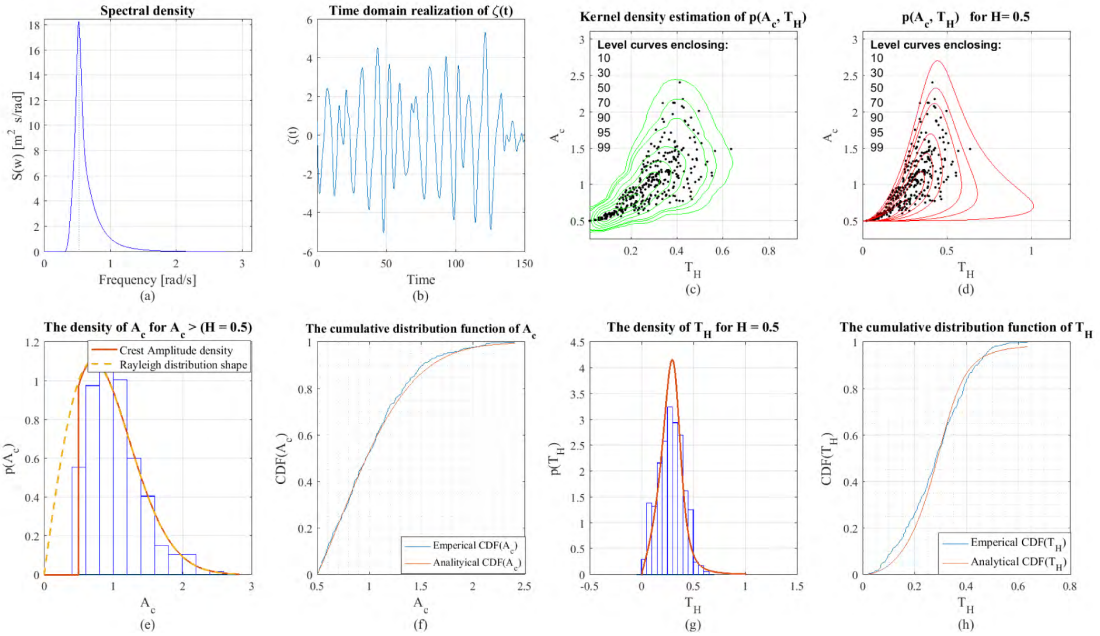

FIGURE 12. Time domain simulation of real sea data for normalized threshold $H = 0.5$, $H_S = 8\ m$ and $T_P = 12\ s$; (a) depicts the spectral density, (b) is a portion of the related time domain realization; black dots in (c) are crest amplitudes greater than $H = 0.5$ and related excursion duration; green curves are the obtained kernel density estimation of $p(A_c, T_H)$; (d) shows the proposed theoretical formula for $p(A_c, T_H)$ Eq. (20); (e:f) are the marginal distributions for crest amplitude and excursion duration, respectively.

peak period $T_P = 12\ s$ (modelled by a JONSWAP spectrum), for more than $1e + 6$ points in time domain for different threshold, Figs. 12 to 14. Poor performance of estimated excursion duration distribution for $H = 0.5$ —which is more evident in Fig. 12 part (h) —is because of the fact that narrow-band assumption is not valid here. This is evident from time domain realization Fig. 12 part (b), i.e., having more than one maximum/minimum between each zero-up/down crossing and successive zero-down/up crossing.

A closer look at sea states spectral density, reveals that the trend for higher level H is similar to narrower spectrum (smaller ν values), since a smaller portion of the frequencies covered by the spectrum have enough energy, those are closer to peak-frequency, to cross the higher level. Consequently, by increasing level H the proposed joint distribution and its marginal distributions are closer to simulation results and have a better performance, Figs. 13 and 14. This is more evident by comparing parts (g) and (h) of Figs. 12 – 14. It is also noticeable that by increasing H, the correlation between crest amplitude and excursion period increases, Fig. 14

Simulation of real sea data for normalized threshold $H = 1$, $H_s = 8\ m$ and $T_p = 12\ s$. (a) depicts the spectral density, (b) is a portion of the related time domain realization; black dots in (c) are crest amplitudes greater than H and related excursion duration and green curves are the obtained kernel density estimation of $p(A_c, T_H)$; (d) shows the proposed theoretical formula for $p(A_c, T_H)$ Eq. (20); (e:f) are the marginal distributions for crest amplitude and excursion period, respectively.

Besides the visual inspection of the proposed distributions and simulated data, it is critical to provide a quantitative accuracy metric using Goodness-of-fit (GoF) test. There are many GoF tests, while, empirical distribution function (EDF)-based tests such as the Kolmogorov-Smirnov (K-S) and Anderson-Darling (A-D) tests are often found to be more powerful than the Chi-square test [31]–[33]. A-D test is especially useful where it is needed to places more weight or discrimination power at the tails of the distribution which is very useful for heavy-tail distribution [34]; hence, K-S test is used here. Related test statistics for different significance level α are presented in Tables 2 and 3.

The $sup|ECDF - CDF|$ refers to the maximum deviation between empirical cumulative distribution function (ECDF) and the proposed marginal distribution for excursion duration T_H as well as crest amplitude A_c. To pass the K-S test, this

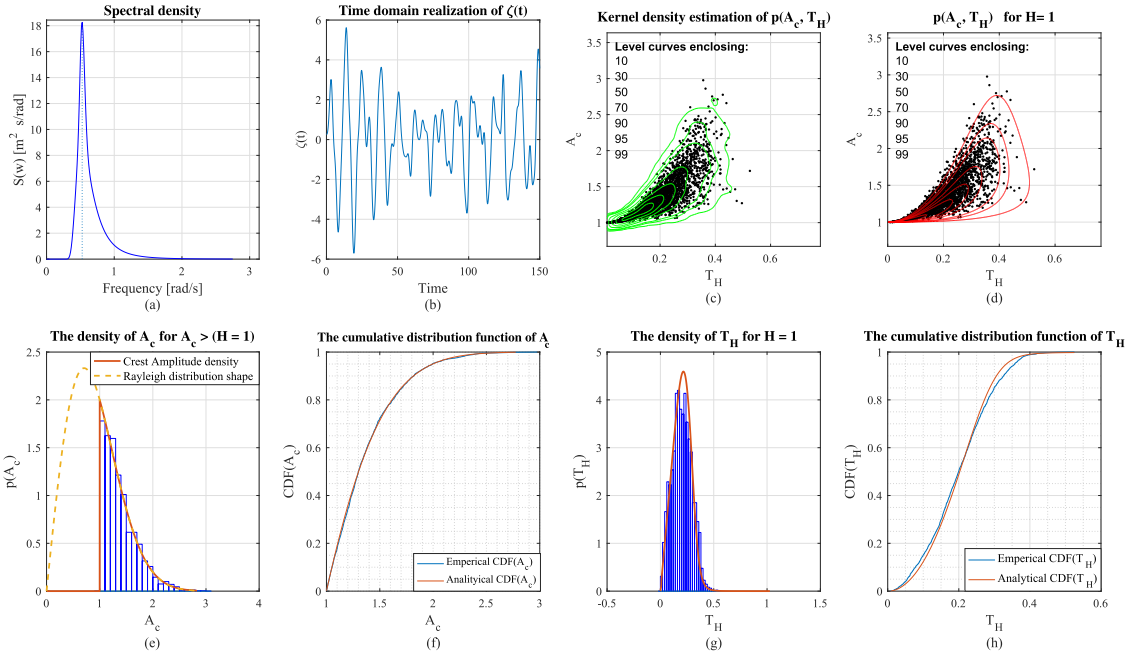

FIGURE 13. Simulation of real sea data for normalized threshold $H = 1$, $H_S = 8\ m$ and $T_P = 12\ s$. (a) depicts the spectral density, (b) is a portion of the related time domain realization; black dots in (c) are crest amplitudes greater than H and related excursion duration and green curves are the obtained kernel density estimation of $p(A_c, T_H)$; (d) shows the proposed theoretical formula for $p(A_c, T_H)$ Eq. (20); (e:f) are the marginal distributions for crest amplitude and excursion period, respectively.

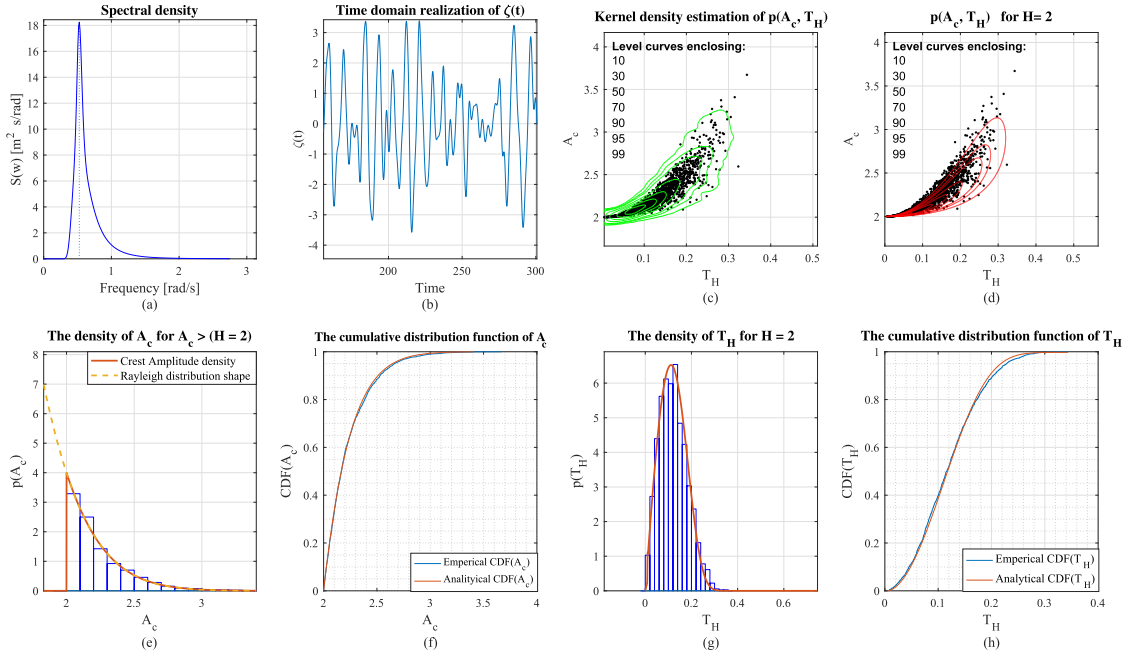

FIGURE 14. Simulation of real sea data for normalized threshold $H = 2$, $H_S = 8\ m$ and $T_P = 12\ s$. (a) depicts the spectral density, (b) is a portion of the related time domain realization; black dots in (c) are crest amplitudes greater than H and related excursion duration and green curves are the obtained kernel density estimation of $p(A_c, T_H)$; (d) shows the proposed theoretical formula for $p(A_c, T_H)$ Eq. (20); (e:f) are the marginal distributions for crest amplitude and excursion period, respectively.

deviation must be smaller, for a given significance level α, than the related critical value D_n^α —n is the sample size. For example, in Table 2 the first column for T_H, the test statistics is 0.0585 and is smaller than $D_n^{\alpha=0.01} = 0.0607$ and $D_n^{\alpha=0.001} = 0.0726$ which means the proposed formula in this case passed the K-S test with significance level equal to $\alpha = 0.01$ and 0.001. It is seen that for $\nu = 0.5$ and $H = 0.5$, the proposed distribution function for T_H faced at the maximum 5.66% error with the confidence level of $1 - \alpha = 99\%$ or faced 6.77% error with the confidence level

TABLE 2. K-S test statistics for ideal narrow-band Gaussian process for different ν and H values.

K-S test statistics for Ideal Narrow-band Gaussian process		H=0.5					H=1	H=2
		$\nu=0.1$	$\nu=0.2$	$\nu=0.3$	$\nu=0.4$	$\nu=0.5$	$\nu=0.5$	$\nu=0.5$
Critical values D_n^α at significance level α	$\alpha=0.10$	0.0455	0.0448	0.0443	0.0437	0.0423	0.0315	0.0378
	$\alpha=0.05$	0.0507	0.0499	0.0494	0.0487	0.0472	0.0351	0.0431
	$\alpha=0.01$	0.0607	0.0598	0.0592	0.0584	0.0566	0.0421	0.0481
	$\alpha=0.001$	0.0726	0.0715	0.0708	0.0699	0.0677	0.0504	0.0689
$Sup\lvert ECDF(T_H)-CDF(T_H)\rvert$		0.0585	0.0515	0.0517	0.0425	0.0431	0.0284	0.0296
Critical values D_n^α at significance level α	$\alpha=0.10$	0.0435	0.0437	0.0427	0.0424	0.0410	0.0303	0.0264
	$\alpha=0.05$	0.0485	0.0487	0.0476	0.0473	0.0457	0.0338	0.0301
	$\alpha=0.01$	0.0582	0.0584	0.0571	0.0567	0.0547	0.0405	0.0335
	$\alpha=0.001$	0.0696	0.0699	0.0683	0.0678	0.0654	0.0485	0.402
$Sup\lvert ECDF(A_c)-CDF(A_c)\rvert$		0.0332	0.0200	0.0276	0.0290	0.0399	0.0188	0.0213

TABLE 3. K-S test statistics for different sea states and H values.

K-S test statistics for different sea states		Site1- Atlantic : Hs=8,Tp=12, Water depth = 40m, nu=0.3660			Site2- North sea : Hs=13.5,Tp=13, Water depth = 200m, nu=0.3247			Site3- North sea : Hs=8,Tp=10, Water depth = 40m, nu=0.3267		
		H=0.5	H=1	H=2	H=0.5	H=1	H=2	H=0.5	H=1	H=2
Critical values D_n^α at significance level α	$\alpha=0.10$	0.0719	0.0320	0.0408	0.0720	0.0326	0.0413	0.0632	0.0345	0.0399
	$\alpha=0.05$	0.0801	0.0357	0.0455	0.0803	0.0364	0.0460	0.0704	0.0384	0.0445
	$\alpha=0.01$	0.0960	0.0427	0.0545	0.0962	0.0436	0.0551	0.0844	0.0461	0.0533
	$\alpha=0.001$	0.1149	0.0511	0.0653	0.1151	0.0521	0.0660	0.1017	0.0551	0.0637
$Sup\lvert ECDF(T_H)-ACDF(T_H)\rvert$		0.0809	0.0483	0.0219	0.1053	0.0471	0.0351	0.0926	0.0485	0.0238
Critical values D_n^α at significance level α	$\alpha=0.10$	0.0710	0.0308	0.0241	0.0714	0.0640	0.0257	0.0634	0.0193	0.0212
	$\alpha=0.05$	0.0792	0.0343	0.0274	0.0796	0.0714	0.0293	0.0707	0.0220	0.0242
	$\alpha=0.01$	0.0949	0.0412	0.0306	0.0954	0.0856	0.0326	0.0847	0.0246	0.0270
	$\alpha=0.001$	0.1120	0.0493	0.0307	0.1141	0.1024	0.0391	0.1013	0.0294	0.0365
$Sup\lvert ECDF(A_c)-ACDF(A_c)\rvert$		0.0520	0.0127	0.0300	0.858	0.0329	0.0186	0.0301	0.0095	0.0115

of $1-\alpha=99.9\%$, and for the density function of A_c, there is 5.47% and 6.54% error for confidence level 99% and 99.9%, respectively.

Similar results for the three aforementioned European offshore sites are presented in Table 3. It should be noted that the higher the level H is the longer simulation time is required to obtain a more accurate error band, since fewer excursion happens by increasing H; therefore, presented results pertinent to $H=2$ in Tables 2 and 3 are conservative, which it is evident from higher differences between D_n^α and test statistics for $H=2$. It is also seen that by increasing the threshold level H, especially for sea states, the accuracy of the proposed distribution increase. One of the most valuable features of the K-S two-sided test statistic is that for a significance level α, its critical value D_n^α may be used to form a confidence band for the true unknown distribution function, [35, Ch.6]. The upper and lower confidence band, for a significance level α, is defined as

$$\begin{aligned} U(x) &= CDF(x)+D_n^\alpha \quad \text{if } CDF(x)+D_n^\alpha \le 1 \\ U(x) &= 1 \quad \text{if } CDF(x)+D_n^\alpha > 1 \\ L(x) &= CDF(x)-D_n^\alpha \quad \text{if } CDF(x)+D_n^\alpha \ge 0 \\ L(x) &= 0 \quad \text{if } CDF(x)-D_n^\alpha < 0 \end{aligned} \tag{31}$$

Taking into account the K-S test results, Tables 2 and 3, and Eq. (31), the error band between simulated data and proposed distributions with confidence level of 99.9% or 99% is quite acceptable, and for the threshold levels greater or equal than $\frac{1}{\sqrt{2m_0}}$—normalized threshold $H \ge 1$—even for a wide band spectrum the proposed formula has almost 5% error.

IV. CONCLUSION

An analytical approximate of the joint distribution of wave amplitude and excursion duration was derived for a narrow-band Gaussian process $\zeta(t)$ with the level H as a parameter. Salient features of the proposed formula included that only information of the three lowest spectral moments (m_0, m_1, m_2) are needed to construct the joint distribution. Ideal narrow-band spectra and three real sea state spectra were used to provide a simulation-based validation. The joint distribution of crest amplitude and excursion duration was compared with a non-parametric piecewise density estimator, the Kernel Density Estimation (KDE). It was shown that the proposed joint distribution agreed well with the KDE. The accuracy of the proposed formula was also validated quantitatively using a Kolmogorov-Smirnov (K-S) goodness-of-fit test; the small error bands between the proposed model and simulation data showed the accuracy of the marginal distributions: crest excursion amplitude, $p(A_c)$, and duration of excursion, $p(T_H)$. The accuracy of the marginal distributions was shown to decrease when spectra become broad band. Moreover, for a spectrum representing sea state, the accuracy was shown to increase for increasing level H, in that only a small portion of frequencies—those are close to peak frequency—have enough power to cross the higher H levels, which is similar to have a narrower spectrum. The paper contributes with an analytic solution for the density of excursion

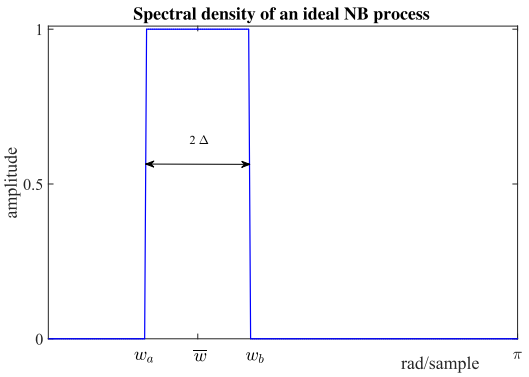

FIGURE 15. Ideal Narrow-band spectral density.

and duration of high loads, which could supplement or even replace existing empirical approaches.

APPENDIX

A. IDEAL NARROW-BAND SPECTRUM PROPERTIES

The objective of this section is to generate an ideal NB spectrum and examine the relation between spectral width parameter ν, $\bar{w}$ as mean frequency, and cut-in and cut-off frequency, w_a and w_b respectively, Fig. 15.

Fig. 15 depicts an ideal NB spectrum, it can be easily shown that $\mu_0 = \omega_b - \omega_a$ and $\mu_2 = \frac{1}{3}(\omega_b - \bar{\omega})^3 - \frac{1}{3}(\omega_a - \bar{\omega})^3$, so based on Eq. (7) we have

$$\Delta = \sqrt{3}\,\nu\,\bar{\omega}. \tag{32}$$

On the other hand $\bar{\omega} - \Delta = \omega_a$ must be positive, so $\sqrt{3}\nu < 1$ which results in $\nu < 1/sqrt(3) = 0.5774$; accordingly in our simulation ν takes values equal or less than 0.5. Higher $\bar{\omega}$ value for a given spectral width parameter ν results in wider spectrum. Choice of $\bar{\omega}$ indicates the relation between mean sampling frequency and Nyquist frequency. In many applications, it is viable to assume that Nyquist frequency is ten times higher than the mean frequency; however, in our simulation we assumed $\bar{\omega} = 0.6$ to have a wider range of spectrum to check the performance of the proposed formula for quiet wide spectra.

B. DERIVATION OF $K(H, \nu)$

Here we derive the normalization factor Eq. (25).

$$\int_H^\infty K(H,\nu)\,2A_c \exp\left(-A_c^2\right)\frac{L(\nu)}{2}\left[1+\operatorname{erf}\left(\frac{A_c}{\nu}\right)\right]dx = 1$$

$$\Rightarrow \frac{1}{K(H,\nu)} \times \frac{2}{L(\nu)}$$

$$= \int_H^\infty 2A_c \exp\left(-A_c^2\right)\left[1+\operatorname{erf}\left(\frac{A_c}{\nu}\right)\right]dA_c \tag{33}$$

by expanding the integral we have

$$\frac{1}{K(H,\nu)} \times \frac{2}{L(\nu)}$$

$$= \int_H^\infty 2A_c \exp\left(-A_c^2\right)dA_c$$

$$+ \int_H^\infty 2A_c \exp\left(-A_c^2\right)\operatorname{erf}\left(\frac{A_c}{\nu}\right)dA_c$$

$$= \exp(-H^2) + \frac{1}{\sqrt{\nu^2+1}}\cdot$$

$$\left[1+\exp(-H^2)\operatorname{erf}\left(\frac{H}{\nu}\right)\sqrt{\nu^2+1} - \operatorname{erf}\left(\frac{H\sqrt{\nu^2+1}}{\nu}\right)\right] \tag{34}$$

Replacing $L(\nu)$ from Eq. (10), we end up with the following expression for $K(H, \nu)$

$$K(H,\nu) = \frac{1+\sqrt{\nu^2+1}}{1+\exp(-H^2)\sqrt{\nu^2+1}\left(1+\operatorname{erf}\left(\frac{H}{\nu}\right)\right) - \operatorname{erf}\left(\frac{H+\sqrt{\nu^2+1}}{\nu}\right)}. \tag{35}$$

ACKNOWLEDGMENT

This work has been carried out at the Center for Autonomous Marine Operations and Systems (AMOS) and Center for Ships and Ocean Structures (CeSOS). The Norwegian Research Council is acknowledged as the main sponsor of AMOS and CeSOS. The first author would like to acknowledge WAFO group, Mathematical Statistics, Centre for Mathematical Sciences, Lund University., for the WAFO open source Matlab toolbox.

REFERENCES

[1] J. P. Kofoed, P. Frigaard, E. Friis-Madsen, and H. C. Sørensen, "Prototype testing of the wave energy converter wave dragon," *Renew. Energy*, vol. 31, no. 2, pp. 181–189, 2006.
[2] M. K. Ochi, *Applied Probability and Stochastic Processes: In Engineering and Physical Sciences*, vol. 226. Hoboken, NJ, USA: Wiley, 1990.
[3] F. Ramos-Alarcón, V. Kontorovich, and M. Lara, "On the level crossing duration distributions of nakagami processes," *IEEE Trans. Commun.*, vol. 57, no. 2, pp. 542–552, Feb. 2009.
[4] S. O. Rice, "Mathematical analysis of random noise," *Bell Syst. Tech. J.*, vol. 23, no. 3, pp. 282–332, 1944.
[5] S. O. Rice, "Mathematical analysis of random noise," *Bell Syst. Tech. J.*, vol. 24, no. 1, pp. 46–156, 1945.
[6] R. L. Stratonovich, *Topics in the Theory of Random Noise*, vol. 2. Boca Raton, FL, USA: CRC Press, 1967.
[7] M. S. Longuet-Higgins, "On the intervals between successive zeros of a random function," *Proc. Roy. Soc. London A, Math. Phys. Sci.*, vol. 246, no. 1244, pp. 99–118, 1958.
[8] M. S. Longuet-Higgins, "The distribution of intervals between zeros of a stationary random function," *Philos. Trans. Roy. Soc. London A, Math., Phys. Eng. Sci.*, vol. 254, no. 1047, pp. 557–599, 1962.
[9] M. S. Longuet-Higgins, "The effect of non-linearities on statistical distributions in the theory of sea waves," *J. Fluid Mech.*, vol. 17, no. 3, pp. 459–480, 1963.
[10] W.-Z. He and M.-S. Yuan, "Statistical property of threshold-crossing for zero-mean-valued, narrow-banded Gaussian processes," *Appl. Math. Mech.*, vol. 22, no. 6, pp. 701–710, 2001.
[11] C. Graham, "The parameterisation and prediction of wave height and wind speed persistence statistics for oil industry operational planning purposes," *Coastal Eng.*, vol. 6, no. 4, pp. 303–329, 1982.
[12] S. Kuwashima and N. Hogben, "The estimation of wave height and wind speed persistence statistics from cumulative probability distributions," *Coastal Eng.*, vol. 9, no. 6, pp. 563–590, 1986.
[13] N. Nigam, *Introduction to Random Vibrations*, vol. 3. Cambridge, MA, USA: MIT Press, 1983.
[14] M. Mathiesen, "Estimation of wave height duration statistics," *Coastal Eng.*, vol. 23, nos. 1–2, pp. 167–181, 1994.
[15] Y. K. Belyaev and V. P. Nosko, "Characteristics of excursions above a high level for a Gaussian process and its envelope," *Theory Probab. Appl.*, vol. 14, no. 2, pp. 296–309, 1969.

[16] S. M. Berman, "Excursions above high levels for stationary Gaussian processes," *Pacific J. Math.*, vol. 36, no. 1, pp. 63–79, 1971.
[17] S. M. Berman, "Maxima and high level excursions of stationary Gaussian processes," *Trans. Amer. Math. Soc.*, vol. 160, pp. 65–85, Oct. 1971.
[18] S. M. Berman, "A class of limiting distributions of high level excursions of Gaussian processes," *Probab. Theory Rel. Fields*, vol. 21, no. 2, pp. 121–134, 1972.
[19] M. Kratz *et al.*, "Level crossings and other level functionals of stationary Gaussian processes," *Probab. Surv.*, vol. 3, no. 1, pp. 230–288, 2006.
[20] D. R. Morgan, "On level-crossing excursions of Gaussian low-pass random processes," *IEEE Trans. Signal Process.*, vol. 55, no. 7, pp. 3623–3632, Jul. 2007.
[21] V. M. Nguyen. (May 2012). "Some properties of large excursions of a stationary Gaussian process." [Online]. Available: https://arxiv.org/abs/1205.4126
[22] R. A. Wooding, "Approximate joint probability distribution for wave amplitude and frequency in random noise," *Nature*, vol. 176, no. 4481, pp. 564–565, 1955.
[23] A. Cavanie, X. Arhan, and X. Ezraty, "A statistical relationship between individual heights and periods of storm waves," in *Proc. Conf. Behav. Offshore Struct.*, Trondheim, Norway, 1976, pp. 354–360.
[24] M. S. Longuet-Higgins, "On the joint distribution of the periods and amplitudes of sea waves," *J. Geophys. Res.*, vol. 80, no. 18, pp. 2688–2694, 1975.
[25] M. S. Longuet-Higgins, "On the joint distribution of wave periods and amplitudes in a random wave field," *Proc. Roy. Soc. A, Math., Phys. Eng. Sci.*, vol. 389, no. 1797, pp. 241–258, 1983.
[26] E. Antão and C. G. Soares, "Joint distributions of wave steepness in narrow band sea states," *Ocean Eng.*, vol. 101, pp. 201–210, Jun. 2015.
[27] J. L. Lawson and G. E. Uhlenbeck, *Threshold Signals*. New York, NY, USA: McGraw-Hill, 1950.
[28] N. M. Blachman, "On fourier series for Gaussian noise," *Inf. Control*, vol. 1, no. 1, pp. 56–63, 1957.
[29] R. S. Kota, "Wave loads on decks of offshore structures in random seas," Ph.D. dissertation, Dept. Marine Technol., Norwegian Univ. Sci. Technol., Trondheim, Norway, 2012.
[30] L. Li, Z. Gao, and T. Moan, "Joint environmental data at five european offshore sites for design of combined wind and wave energy devices," in *Proc. ASME 32nd Int. Conf. Ocean, Offshore Arctic Eng.*, 2013, p. V008T09A006.
[31] S. Hansen and M. Blanke, "Diagnosis of airspeed measurement faults for unmanned aerial vehicles," *IEEE Trans. Aerosp. Electron. Syst.*, vol. 50, no. 1, pp. 224–239, Jan. 2014.
[32] M. J. Slakter, "A comparison of the pearson chi-square and Kolmogorov goodness-of-fit tests with respect to validity," *J. Amer. Stat. Assoc.*, vol. 60, no. 311, pp. 854–858, 1965.
[33] M. Ghane, A. R. Nejad, M. Blanke, Z. Gao, and T. Moan, "Statistical fault diagnosis of wind turbine drivetrain applied to a 5 MW floating wind turbine," *J. Phys., Conf. Ser.*, vol. 753, no. 5, p. 052017, 2016.
[34] A. H.-S. Ang and W. H. Tang, *Probability Concepts in Engineering: Emphasis on Applications to Civil and Environmental Engineering*. Hoboken, NJ, USA: Wiley, 2007.
[35] W. J. Conover, *Practical Nonparametric Statistics*, 3rd ed. Hoboken, NJ, USA: Wiley, 1999.

MAHDI GHANE was born in Mashhad, Iran, in 1984. He received the B.Sc. degree in electrical engineering from Ferdowsi University, in 2007, and the M.Sc. degree in mechatronics from the K. N. Toosi University of Technology, Tehran, Iran, in 2009. He is currently pursuing the Ph.D. degree with the Center for Autonomous Marine Operations and Systems, Norwegian University of Science and Technology, Trondheim, Norway. In 2014, he spent 6 months as a Ph.D. Student Researcher involved in fault detection and signal processing with Electrical Engineering Department, The University of Melbourne. His current research interests include fault detection and identification, renewable energy, and system modeling.

ZHEN GAO received the M.Sc. degree in naval architecture and ocean engineering from Shanghai Jiao Tong University in 2003 and the Ph.D. degree in marine technology from the Norwegian University of Science and Technology (NTNU) in 2008. From 2008 to 2014, he worked as a Post-Doctoral Researcher and then as an Adjunct Associate Professor with the Offshore Wind Energy Group led by Prof. T. Moan, before he became a Full Professor with NTNU in 2015. His research areas include coupled dynamic analysis of offshore renewable energy devices and marine operations related to transport and installation of offshore wind turbines. He serves as an Editorial Board Member for several international journals, including *Marine Structures* and*Journal of Offshore Mechanics and Arctic Engineering*.

MOGENS BLANKE received the M.Sc. and Ph.D. degrees in electrical engineering from the Technical University of Denmark (DTU), Lyngby, Denmark, in 1974 and 1982, respectively. He was a Systems Analyst with the European Space Agency from 1975 to 1976, the Head of Marine Division, a Lyngsø Marine, Denmark, from 1985 to1990, and a Full Professor with Aalborg University from 1990 to 1999. He has been a Professor in automation and control with DTU since 2000. Since 2005, he has been an Adjunct Professor with the Center for Excellence of Autonomous Marine Operations and Systems, Norwegian University of Science and Technology, Trondheim, Norway. He has authored over 270 scientific papers, book chapters, and books, including a widely recognized textbook on *Diagnosis and Fault-tolerant Control*. His research interests include general subjects in automation and control, fault diagnosis and prognosis, and fault tolerant control systems. He has been a Technical Editor for the IEEE Transactions on Aerospace and Electronic Systems and a dedicated editor for several special issues of journals. He is currently an Associate Editor for *Control Engineering Practice*.

TORGEIR MOAN received the M.Sc. and Ph.D. degrees in civil engineering from the Norwegian University of Science and Technology (NTNU), Trondheim, Norway, in 1968 and 1976, respectively. He has been a Professor of marine structures with NTNU since 1977 and the Director of the Center for Ships and Ocean Structures with NTNU since 2002. He was a Visiting Professor with the Massachusetts Institute of Technology and University of California at Berkeley, Berkeley, CA, USA, and a part-time Adjunct (Keppel) Professor with the National University of Singapore, Singapore. He has authored over 600 scientific papers, delivered over 40 keynote, plenary lectures in international conferences and award lectures, and supervised over 80 Ph.D. candidates. His research interests include stochastic dynamic modeling, analysis, and reliability of marine structures, and his current research focus is on facilities for offshore wind and wave energy conversion. He is a member of the Norwegian Academy of Science and Letters and a Fellow of the Royal Academy of Engineering and several international professional societies. He is the Editor of the *Journal of Marine Structures* and serves on the editorial board of a number of international journals. He has received numerous research prizes.